JOURNAL OF SOLID STATE CHEMISTRY **139,** 347–355 (1998)
ARTICLE NO. SC987856

Modulated Structures of Homologous Compounds $InMO_3(ZnO)_m$ (M = In, Ga; m = Integer) Described by Four-Dimensional Superspace Group

Chunfei Li,[1] Yoshio Bando, Masaki Nakamura, Mitsuko Onoda, and Noboru Kimizuka*

*National Institute for Research in Inorganic Materials, 1-Namiki, Tsukuba, Ibaraki 305, Japan; and *Universidad de Sonora, CIPM, Hermosilo, Sonora, C.P. 83000, Mexico*

Received December 30, 1997; in revised form April 8, 1998; accepted April 9, 1998

The modulated structures appearing in the homologous compounds $InMO_3(ZnO)_m$ (M = In, Ga; m = integer) were observed by using a high-resoultion transmission electron microscope and are described based on a four-dimensional superspace group. The electron diffraction patterns for compounds with m larger than 6 reveal extra spots, indicating the formation of a modulated structure. The subcell structures for m = odd and even numbers are assigned to be either monoclinic or orthorhombic, respectively. On the other hand, extra spots can be indexed by one-dimensional modulated structure. The possible space groups for the subcell structure are Cm, $C2$, and $C2/m$ for m = odd numbers, while those for m = even numbers are $Ccm2_1$ and $Ccmm$, respectively. Then, corresponding possible superspace groups are assigned to be P_s^{C2}, $P_{\bar{1}}^{Cm}$, and $P_{s\bar{1}}^{C2/m}$ for odd m numbers and $P_{1\bar{1}\bar{1}}^{Ccm2_1}$ and $P_{1\bar{1}1}^{Ccmm}$ for even m numbers. Based on the superspace group determination, a structure model for a one-dimensional modulated structure is proposed.

1. INTRODUCTION

The homologous compound $In_2O_3(ZnO)_m$ (m = integer) was first found by Cannard and Tilley (1) and Kasper (2). They reported that the homologous compound is a layered structure, consisting of In_2O_3 layers interleaved with m layers of ZnO. Recently, the present authors successfully synthesized a series of homologous compounds, $InMO_3(ZnO)_m$ (M = In, Fe, Ga, and Al; m = integer) (3–6). We proposed a structure model different from that of Kasper, where the structure is built up of a succession of InO_2^{1-} (In–O layer) and $MZn_mO_{m+1}^{1+}$ (M/Zn–O layer) layers along the c axis. The space group was assigned as $R\bar{3}m$ when m is an odd number and is $P6_3/mmc$ when m is an even number. It was assumed that trivalent M atoms in the M/Zn–O layers are in a random distribution, since no extra diffraction spots were observed in the X-ray diffraction patterns (7–10).

[1]To whom correspondence should be addressed.

The extra diffraction spots, however, were observed for $InFeO_3(ZnO)_m$ (m = 6, 13) in the electron diffraction patterns (11). They were located at the nonintegral position relative to the subcell spots, indicating the formation of a modulated structure. In the high-resolution lattice images, the modulated structures were successfully imaged, showing a zig-zag or a wave-like shape contrast present only at the Fe/Zn–O layer (11). A further study of elemental analysis using a 300-kV field emission analytical electron microscope revealed that the trivalent Fe atoms were enriched in the zig-zag-shaped regions (12). It was then established that the modulated structure was due to the ordering of the trivalent Fe atoms in the Fe/Zn–O layer. The modulated structures were also observed in another systems of $In_2O_3(ZnO)_m$ (m = 6, 10, 13, 15, 17, and 20) (13). The image contrast of the modulated structures observed was very similar to that of $InFeO_3(ZnO)_m$, while the periodicity and shape were different from each other. In the previous studies, however, a superspace group approach of the modulated structure had not been determined.

A superspace group approach is very useful in describing features of the modulated structure in detail. Wollf *et al.* developed the superspace group description for the modulated structure, where diffraction spots can be indexed as $ha^* + kb^* + lc^* + \sum m_i q_i$. Here, a^*, b^*, and c^* are the lattice vectors in the reciprocal space for the subcell structure and $q_i = \alpha_i a^* + \beta_i b^* + \gamma_i c^*$ is the modulation wavevector (14–17). According to the numbers of i, the modulation is called as one-two-, and n-dimensional modulated structures.

In this paper, the modulated structures of $In_2O_3(ZnO)_m$ (m = 6, 7, 15, and 19) and $InGaO_3(ZnO)_{15}$ are studied by high-resolution electron microscopy and described with a superspace group approach. The subcell spots in the electron diffraction pattern are indexed by either a monoclinic or an orthorhombic cell for m = odd and even numbers, respectively. The extra spots can be indexed as $ha^* + kb^* + lc^* + mq$ by introducing a one-dimensional

0022-4596/98 $25.00

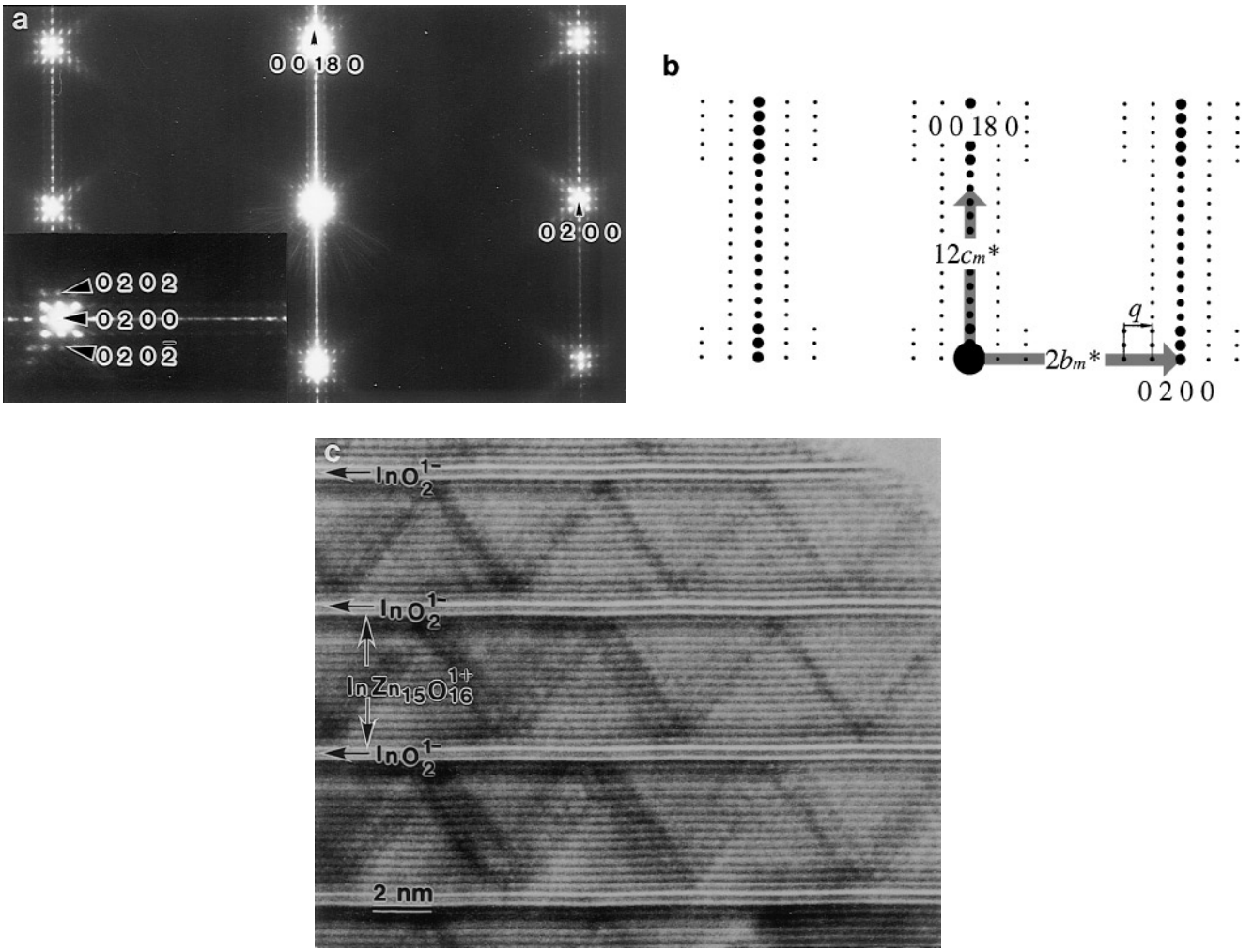

FIG. 1. Electron diffraction pattern showing a b^*_m–c^*_m reciprocal section (a), schematic drawing of (a), and corresponding high-resolution image (c) of $In_2O_3(ZnO)_{15}$. A part of the diffraction spot around (0200) is enlarged with a rotation of 90°.

modulation wavevector, $q = b^*/s$. The possible space groups for subcells and corresponding superspace groups for the modulated structures are then derived. Based on the superspace group, a modulated structure model is proposed.

2. EXPERIMENTAL

A solid-state reaction method was used for sample preparation. The powders of In_2O_3, Ga_2O_3, and ZnO were weighed for each m number and heated in Pt-sealed tube at 1523 K for about 7 days; then they were rapidly cooled down to room temperature. No detectable reactions between the Pt tubes and the samples were observed.

For electron microscope observations, the samples were crushed in an agate mortar and dispersed onto a holey carbon grid by using CCl_4 solution. Selected area electron diffraction patterns and corresponding lattice images were observed by a high-resolution electron microscope (JEM-2000EX), operated at 200 kV.

3. RESULTS AND DISCUSSION

A typical electron diffraction pattern and the corresponding high-resolution lattice image of the modulated structure for $In_2O_3(ZnO)_{15}$ are shown in Fig. 1. In the electron diffraction pattern, both the subcell and extra spots are observed. In the previous study, the subcell spots were indexed by either $R\bar{3}m$ (m = odd numbers) or $P6_3/mmc$ (m = even numbers) (4–6). However, in the present study, they can be well indexed by a monoclinic or an orthorhombic cell, while the extra spots are assigned to the following superspace group description. The subcell spots in Fig. 1a are indexed as $ha^*_m + kb^*_m + lc^*_m$ by considering a monoclinic cell, and the extra spots as $ha^*_m + kb^*_m + lc^*_m + mq$ with $q = b^*_m/s$. Figure 1b is a schematic drawing of Fig. 1a, where

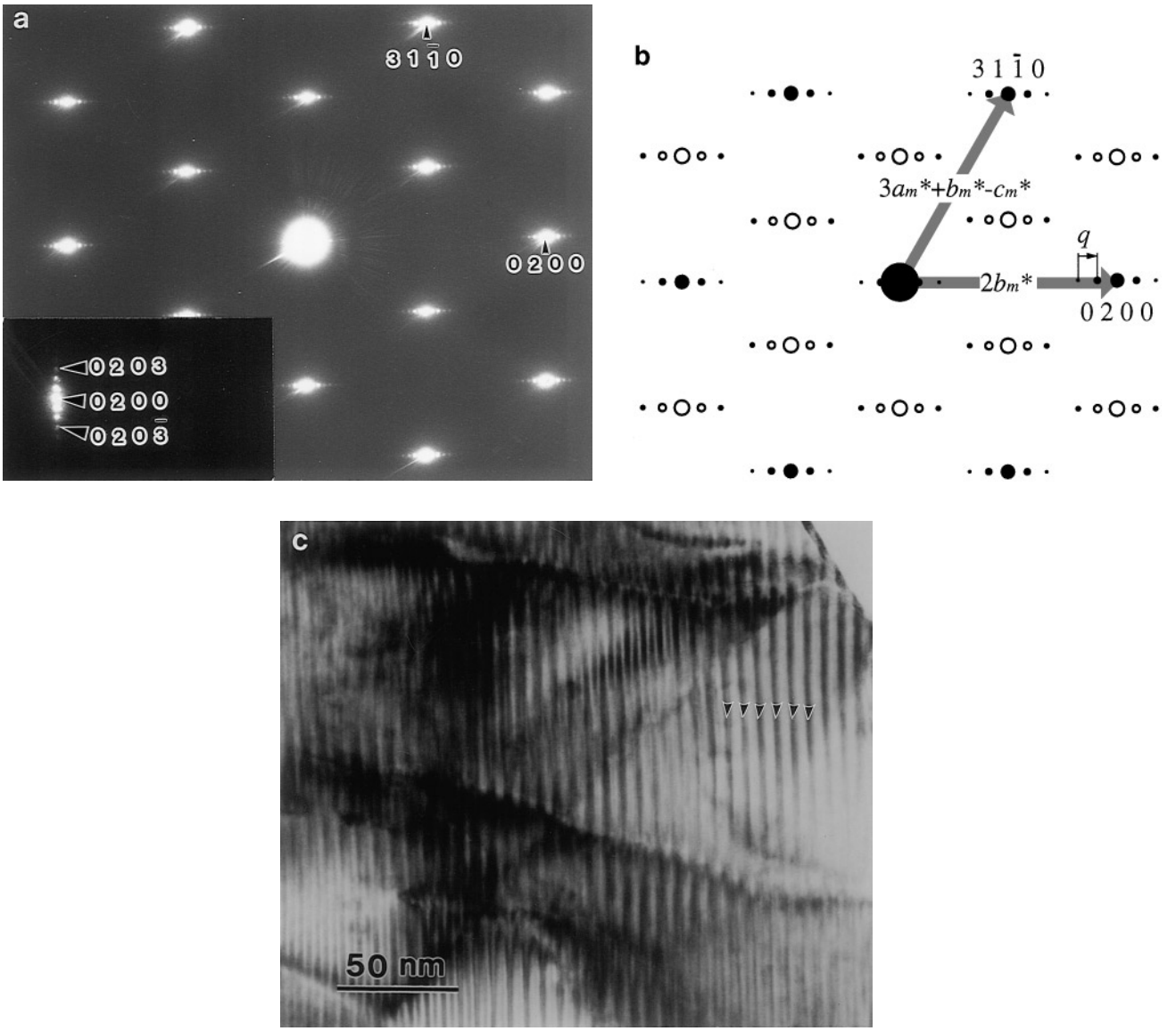

FIG. 2. Electron diffraction pattern taken with the incident electron beam parallel to c_m^* (a), schematic drawing (b), and corresponding image (c) of $In_2O_3(ZnO)_{19}$. Inset in (a) is the enlarged diffraction spots around (0200) with a rotation of 90°.

the reciprocal lattice base vectors and the modulation wavevectors are indicated. The parameters for the monoclinic cell and the values of s for the modulation wavevector are summarized in Table 1. From the value of sb, the periodicity of the modulated structure along the b_m direction is estimated to be about 5.0 nm. The image contrast of Fig. 1c is very similar to those of $InFeO_3(ZnO)_{13}$ and $In_2O_3(ZnO)_m$ (m = 13 and 20) reported in previous papers (11, 13), where the In–O and In/Zn–O layers are indicated as InO_2^{1-} and $InZn_{15}O_{16}^{1+}$, respectively. The zig-zag-shaped contrast appearing within the In/Zn–O layer corresponds to the modulated structure. Based on the previous results (11, 13), this zig-zag image contrast is considered to be caused mainly by the ordering of In atoms within the In/Zn–O layers. Since there is no periodic contrast variation in the In–O layers, we consider this layer not to be modulated. The periodicities of the zig-zag shape vary from area to area and range from about 4.9 to 5.5 nm. The nonintegral periodicity is produced as a result of the average of different integral periodicities. In the image, the angle of the zig-zag shape with respect to the In–O layer is assigned to be about 60°.

In Fig. 2 are the electron diffraction pattern and corresponding image of $In_2O_3(ZnO)_{19}$, respectively. This electron diffraction pattern can also be indexed by considering a monoclinic subcell and a modulation wavevector shown

TABLE 1

Lattice Parameters of the Subcell and the Modulated Structure for the Homologous Compounds $In_2O_3(ZnO)_m$ ($m = 6, 7, 15, 19$) and $InGaO_3(ZnO)_{15}$

Specimen	Subcell						Modulated structure
	a (nm)	b (nm)	c (nm)	$\alpha(^\circ)$ (b and c)	$\beta(^\circ)$ (c and a)	$\gamma(^\circ)$ (a and b)	s in $q = b^*/s$
$In_2O_3(ZnO)_6$	0.57	0.33	4.4	90	90	90	7.2
$In_2O_3(ZnO)_7$	0.57	0.33	2.5	90	94	90	8.1
$In_2O_3(ZnO)_{15}$	0.57	0.33	4.5	90	92	90	15.1
$In_2O_3(ZnO)_{19}$	0.57	0.33	5.6	90	92	90	19.3
$InGaO_3(ZnO)_{15}$	0.57	0.33	4.5	90	92	90	33.1

in Table 1. While the incident electron beam is normal to c_m^* in Fig. 1, it is parallel to c_m^* in Fig. 2. Despite such different incident electron beam directions, the satellite spots appeared only in the b_m^* direction in both Fig. 1a and Fig. 2a. It can be then concluded that the present modulation wave is one dimensional along the b^* axis. Figure 2b is the schematic drawing of Fig. 2a, showing the relation between the reciprocal lattice base vector and the modulation wavevector. In the high-resolution image of Fig. 2c, the vertical straight line contrast indicated by arrows corresponds to the modulated structure. The average spacing of these lines is approximately 6 nm, which is in agreement with $sb = 6$ nm measured from the electron diffraction pattern.

As an example of m = odd number, Figs. 3a and 3b show electron diffraction patterns of $In_2O_3(ZnO)_7$, representing b_m^*–c_m^* and a_m^*–c_m^* reciprocal lattice sections, respectively. If the subcell spots in the diffraction patterns be indexed by the rhombohedral cell (expressed in hexagonal form), then the corresponding modulation wavevector should be $q = a_r^*/s + b_r^*/s$, where a_r^* and b_r^* are the basic reciprocal lattice vectors for the rhombohedral form. However, this result does not agree with the superspace group theory, because only the modulation wavevector along the c_h^* direction is allowed for the one-dimesional modulated structure of a hexagonal (rhombohedral) subcell. The subcell spots in Fig. 3 are successfully indexed by the monoclinic cell. On the other hand, the extra spots can be indexed as $ha_m^* + kb_m^* + lc_m^* + mq$. The modulation wavevector $q = b_m^*/s$ is along the unique axis, which is in accordance with superspace group theory. The extinction rules for the subcell spots are hkl: $h + l = 2n$, which leads to possible space groups of $C2$, Cm, and $C2/m$. The intensities of the extra spots indexed as $(0k0m)$ [m = odd number] such as (0201) and $(020\bar{1})$ are very weak compared with others, as seen in Fig. 3a. It is therefore very difficult to judge that these spots are excited due to the double diffraction effect or the ordinary ones. Then, possible extinction rules for the extra spots are either $0k0m$: $m = 2n$ or no condition. The corresponding possible superspace groups are P_1^{C2}, P_s^{C2}, $P_{\bar{1}}^{Cm}$, $P_{1\bar{1}}^{C2/m}$, and $P_{s\bar{1}}^{C2/m}$, which are shown with the same notations proposed by Yamamoto (18). These superspace groups also correspond to P_1^{B2}, P_s^{B2}, $P_{\bar{1}}^{Bm}$, $P_{1\bar{1}}^{B2/m}$, $P_{s\bar{1}}^{B2/m}$, which are proposed by Wolff *et al.* (14).

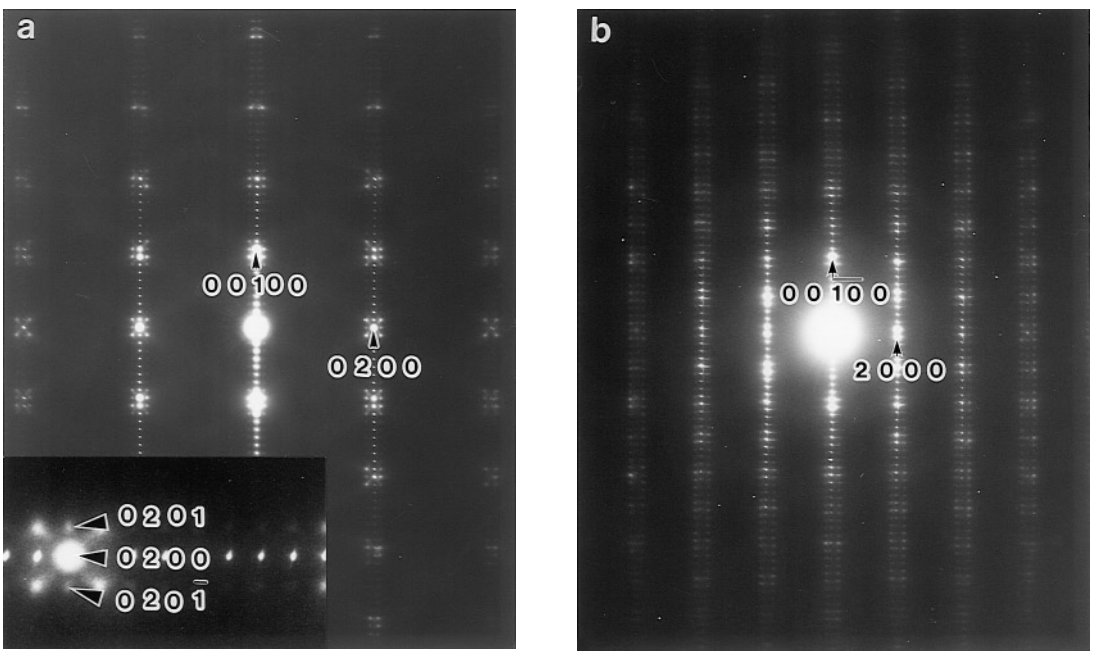

FIG. 3. Electron diffraction patterns of $In_2O_3(ZnO)_7$ showing b_m^*–c_m^* (a) and a_m^*—c_m^* (b) reciprocal sections. A part of the diffraction spot around (0200) is enlarged with a rotation of 90°.

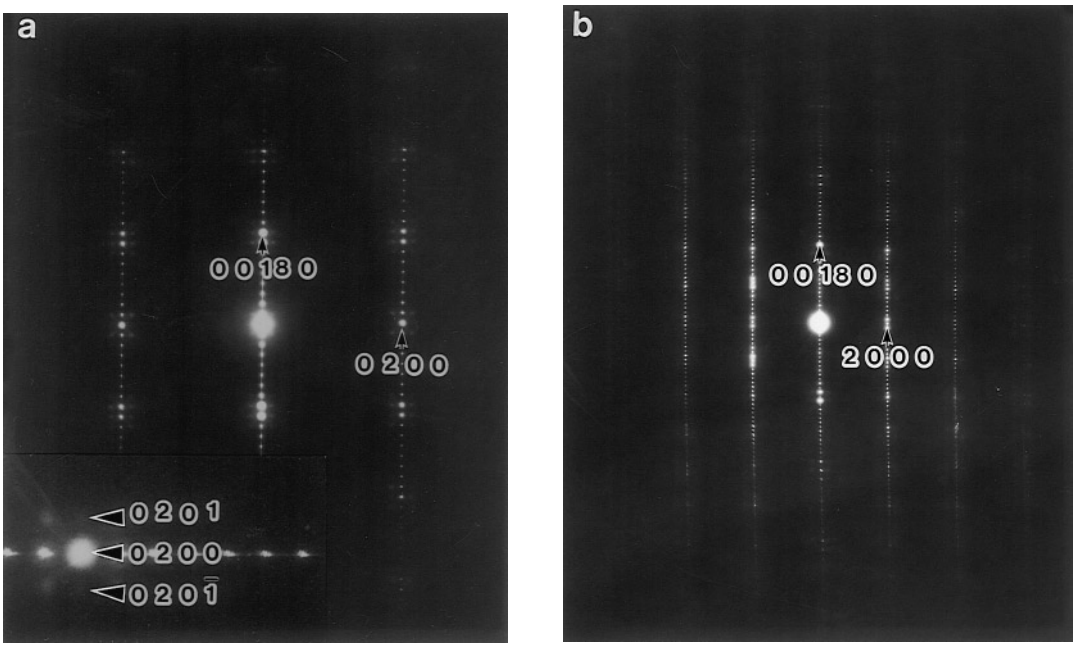

FIG. 4. Electron diffraction patterns of $In_2O_3(ZnO)_6$ showing b_0^*–c_0^* (a) and a_0^*–c_0^* (b) reciprocal sections. A part of the diffraction spot around (0200) is enlarged with a rotation of 90°.

Figures 4a and 4b are electron diffraction patterns of $In_2O_3(ZnO)_6$ as an example of compounds with even m even numbers, showing b_0^*–c_0^* and a_0^*–c_0^* reciprocal lattice sections, respectively. The subcell spots are indexed by the orthorhombic cell instead of the hexagonal one and the result is summarized in Table 1. The extra spots can be indexed as $ha_0^* + kb_0^* + lc_0^* + mq$. The modulation wavevector $q = b_0^*/s$ is along the b_0^* direction. The extinction rules for the subcell spots are hkl: $h + k = 2n$ and $0kl$: $l = 2n$ ($k = 2n$), then the possible space group is either $Ccm2_1$ or $Ccmm$ for the subcell structure. The weak $(00l)$ spots (l = odd number) in the a_0^*–c_0^* section are formed by the double diffraction effect. While no systematic extinctions are observed for the extra spots, it is still in question whether $(0k0m)$ (m = odd number) reflections are forbidden or not, because the intensities of the extra spots such as (0201) and $(020\bar{1})$ in the b_0^*–c_0^* plane are very weak. Then, the extinction rules for the extra spots are either no conditions or $0k0m: k = 2n, m = 2n$. The possible superspace groups are then $P^{Ccm2_1}_{1\bar{1}\bar{1}}$, $P^{Ccmm}_{1\bar{1}1}$, and $P^{Ccmm}_{1\bar{1}s}$, which also correspond to $P^{Cmc2_1}_{\bar{1}1\bar{1}}$, $P^{Ccmm}_{\bar{1}\bar{1}1}$, and $P^{Ccmm}_{\bar{1}\bar{1}s}$ by Yamamoto's notation (18) and $P^{A2_1am}_{\bar{1}1\bar{1}}$, $P^{Amam}_{11\bar{1}}$, and $P^{Amam}_{s1\bar{1}}$ by that of Wolff's *et al.* (14).

Figures 5a and 5b are schematic drawings of reciprocal lattices for compounds with m = odd and even numbers, respectively. The layouts of the subcell spots in Figs. 5a and 5b are very similar to those of rhombohedral $R\bar{3}m$ and hexagonal $P6_3/mmc$, respectively. Three reciprocal lattice vectors, $2a_m^*$, $2b_m^*$, and c_m^*, in (a) correspond to $(1\bar{1}2)$, (110), and (003) of the rhombohedral lattice, while $2a_0^*$, $2b_0^*$, and $2c_0^*$ in (b) correspond to $(1\bar{1}0)$, (110), and (002) of the hexagonal lattice. In both Figs. 5a and 5b, we take the b^* axis as the modulation direction and the c^* axis as the stacking direction of In–O and In/Zn–O layers. In case of m = odd number where the unit cell is monoclinic, b^* is the unique axis. The three reciprocal lattice sections shown in Fig. 5a are $(6a_m^*–2c_m^*)–b_m^*$, $2b_m^*–c_m^*$, and $2a_m^*–c_m^*$. Among them, $(6a_m^*–2c_m^*)–b_m^*$ corresponds to the diffraction pattern of Fig. 2a, $2b_m^*–c_m^*$ those of Figs. 1a and 3a, and $2a_m^*–c_m^*$ that of Fig. 3b. Figure 5b shows $2a_0^*–2b_0^*$, $2b_0^*–2c_0^*$, and $2a_0^*–2c_0^*$ reciprocal lattice sections, of which $2b_0^*–2c_0^*$ corresponds to Fig. 4a and $2a_0^*–2c_0^*$ corresponds to Fig. 4b.

The lattice relations between the monoclinic and rhombohedral cells and between the orthorhombic and hexagonal cells are shown in Figs. 6a and b, respectively. The lattice vectors a_m, b_m, and c_m for the monoclinic cell are related to those of the rhombohedral cell a_r, b_r, and c_r. The relation between them can be expressed by $a_m = a_r - b_r$, $b_m = a_r + b_r$, and $c_m = (a_r - b_r + c_r)/3$. While for the orthorhombic cell, lattice vectors a_0, b_0, and c_0 correspond to the hexagonal cell, a_h, b_h, and c_h, in the relations $a_0 = a_h - b_h$, $b_0 = a_h + b_h$, and $c_0 = c_h$.

Figures 7 and 8 show subcell structures of $InMO_3(ZnO)_7$ (M = In) and $InMO_3(ZnO)_6$ (M = In) as examples of m = odd and even numbers, respectively. The atomic layout was assumed based on both the X-ray diffraction analysis and the results of high-resolution image simulation reported early. In the structures, oxygen atoms are arranged in a hexagonal packing along the $c_m^*(c_0^*)$ axis, in which they are

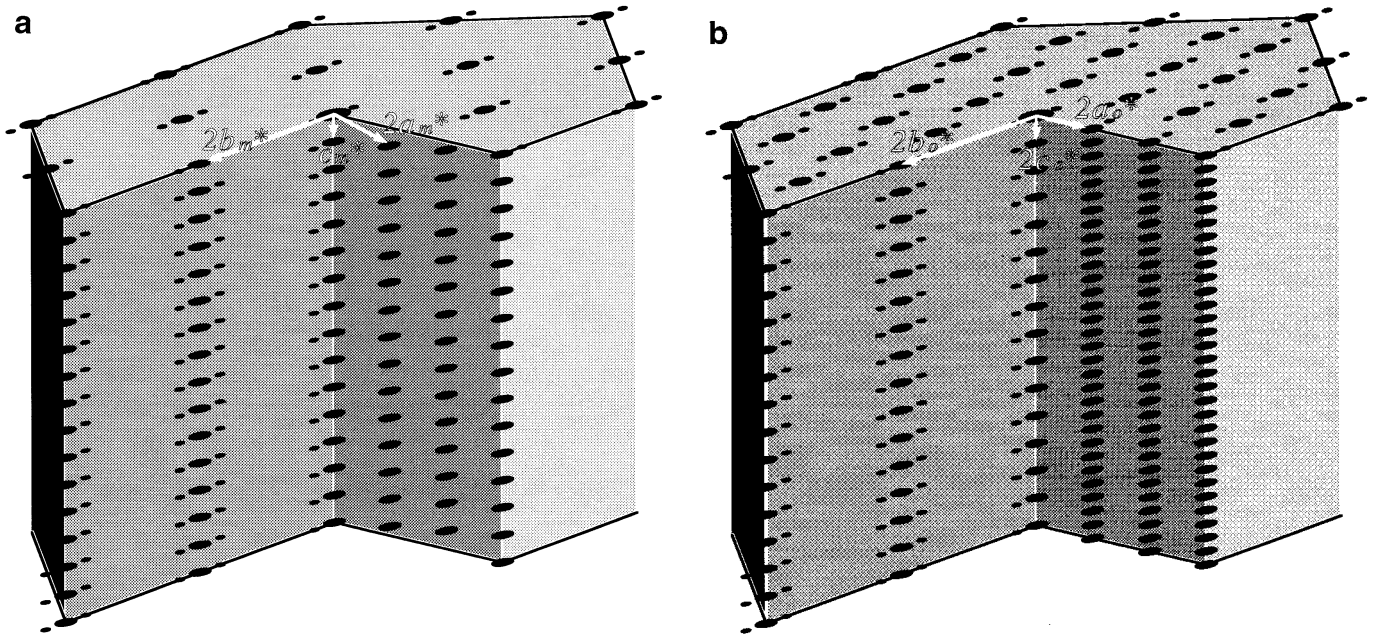

FIG. 5. Schematic drawing of reciprocal lattice of homologous compounds for m = odd (a) and m = even (b) numbers.

stacked as ABAB within the M/Zn–O layer and change into CACA across an In–O layer. The M and Zn atoms occupy either tetragonal or trigonal bypyramidal positions, while In atoms occupy the octahedral positions. For $InMO_3(ZnO)_7$, the structure consisits of In–O layers interleaved with eight layers of M/Zn–O, while in $InMO_3(ZnO)_6$ the In–O layer is sandwiched by seven layers of M/Zn–O.

Figure 9 shows a modulated structure model of $In_2O_3(ZnO)_7$, where the structure is projected along [100] direction of the monoclinic crystal system. For simplicity, the periodicity of the modulated structure sb_m, was assigned as an integer times that of the subcell b_m. Based on the lattice image shown in Fig. 1c, it is assumed that the trivalent M (M = In) atoms in the M/Zn–O layers are ordered to form a single layer of M–O having a zig-zag shape as shown in Fig. 9. The atomic arrangements in the neighboring In/Zn–O layers shift along the [010] direction; for example, the M atom arrangement in the layer indicated as 8 shows a phase shift of approximately π with respect to that of 1. Since the symmetry for the superspace groups of P_1^{C2} and $P_{1\bar{1}}^{C2/m}$ do not show any π shift symmetry for such layers, these two superspace groups can be rejected. Then, the possible superspace groups for compounds with odd m numbers are P_s^{C2}, $P_{\bar{1}}^{Cm}$, and $P_{s\bar{1}}^{C2/m}$. In a similar way, the possible superspace groups can also be assigned as $P_{11\bar{1}}^{Ccm2_1}$ and P_{11s}^{Ccmm} for compounds with even m number, and the structure model for $In_2O_3(ZnO)_6$ is shown in Fig. 10.

It should be pointed out that the above symmetry analysis was performed based on the experimental results of $In_2O_3(ZnO)_m$. Studies of the modulated structures of $InFeO_3(ZnO)_m$ and $InGaO_3(ZnO)_m$ verified that they have the same symmetries as $In_2O_3(ZnO)_m$. As an example, parameters for the subcell and modulated structure of $InGaO_3(ZnO)_{15}$ are shown in Table 1. However, detailed features of the modulated structure, which can be characterized by the angle α of the zig-zag shape with the In–O layer and the periodicity sb, differ from each other. Figure 11 shows the relation of the width of the M/Zn–O layer d, the angle α, and the periodicity sb of the modulated structure. As seen in the high-resolution image of Fig. 1b and that reported in the early paper, angle α depends on the kind of trivalent ion M in the M/Zn–O layer. For example, the value α is almost constant at about 60° for $In_2O_3(ZnO)_m$ (M = In) and about 40° for $InFeO_3(ZnO)_m$ (M = Fe) and $InGaO_3(ZnO)_m$ (M = Ga). Since d is approximately linearly proportional to the m value and sb can be expressed by d as $2d/\tan\alpha$, as shown in Fig. 11, the periodicity for the modulated structures should be linearly proportional to the increase in m numbers. In fact, such linearity is confirmed by the measurement of sb for compounds with different m values from electron diffraction patterns. Figure 12 shows the periodicities of the modulated structures for three different compounds: $In_2O_3(ZnO)_m$ (m = 6,7,10,13,15,17,19,20), $InFeO_3(ZnO)_m$ (m = 6,13), and $InGaO_3(ZnO)_m$ (m = 15). It is clear that the slope of the lines depends on M. The slopes for $InFeO_3(ZnO)_m$ and $InGaO_3(ZnO)_m$ are almost the same. It can be established from Fig. 11 that the periodicity for $InFeO_3(ZnO)_m$ and $InGaO_3(ZnO)_m$ is about twice that of

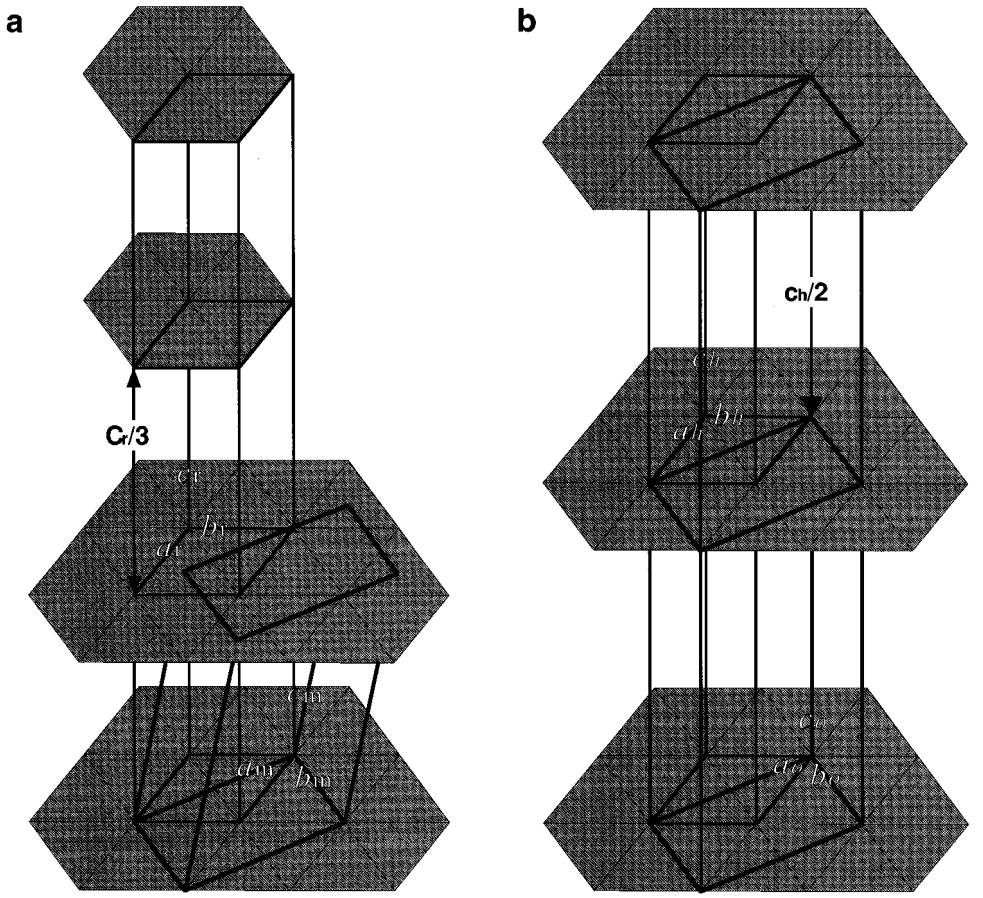

FIG. 6. Lattice relations between the monoclinic and rhombohedral cells (a) and between the orthorhombic and hexagonal cells (b).

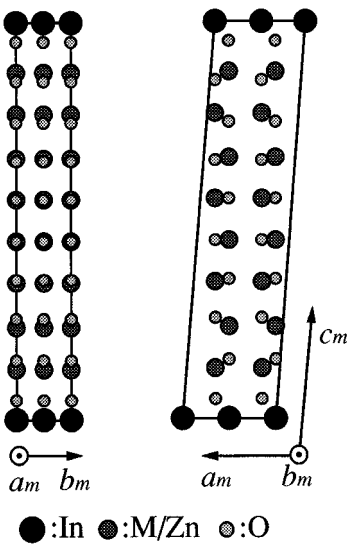

FIG. 7. Subcell structures for $InMO_3(ZnO)_7$ (M = In): The left and right figures are the structure models projected along the [100] and [010] directions, respectively. The large dark circles indicate In atoms, the medium circles, M/Zn, and the small circles, oxygen atoms.

$In_2O_3(ZnO)_m$. This is in good agreement with the ratio of $\tan 60^\circ \tan 40^\circ = 2.1$.

As shown in Figs. 9 and 10, Zn atoms in a wuruzite-type ZnO structure are replaced by one trivalent M atom in the M/Zn–O layer. Since the atomic radii of trivalent M ions are larger than that of Zn ions (19), the introduction of such M ions causes structural stress. It is reasonable to consider that the formation of the modulated structure is related to minimization of this structural stress. The nearest distance between Zn and O in a hypothetical trigonal bipyramidal position is estimated to be about 0.19 nm in ZnO, while the distances between trivalent M and O are about 0.21, 0.20, 0.20, and 0.19 nm for M = In, Fe, Ga, and A1 atoms, respectively. Since the distance for A1 is identical to that of ZnO, there is no structural stress and the modulated structure is not observed in $InAlO_3(ZnO)_m$. For In, Fe, and Ga, the distances are different from ZnO, resulting in the formation of the modulated structure. It should be pointed out that for Fe and Ga the distances are the same, and the angles and periodicities of the modulated structure in $InFeO_3(ZnO)_m$ and $InGaO_3(ZnO)_m$ are identical as shown in Fig. 11.

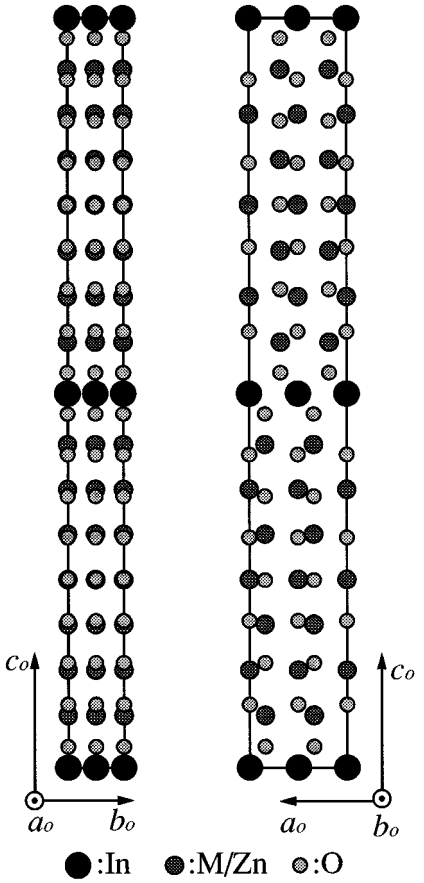

FIG. 8. Subcell structures for $InMO_3(ZnO)_6$ (M = In). The left and right figures are the structure models projected along the [100] and [010] directions, respectively. The symbols are the same as those in Fig. 7.

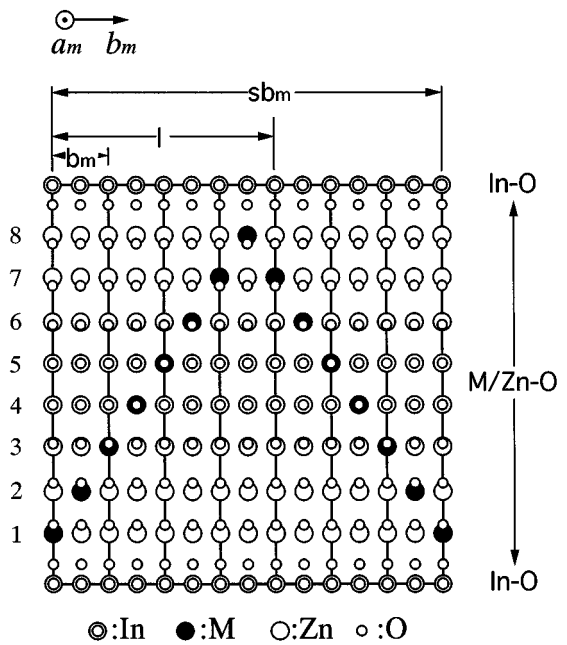

FIG. 9. Modulated structure model of $InMO_3(ZnO)_7$ (M = In). The trivalent In atoms are ordered to form a single In–O layer showing a one-dimensional zig-zag shape.

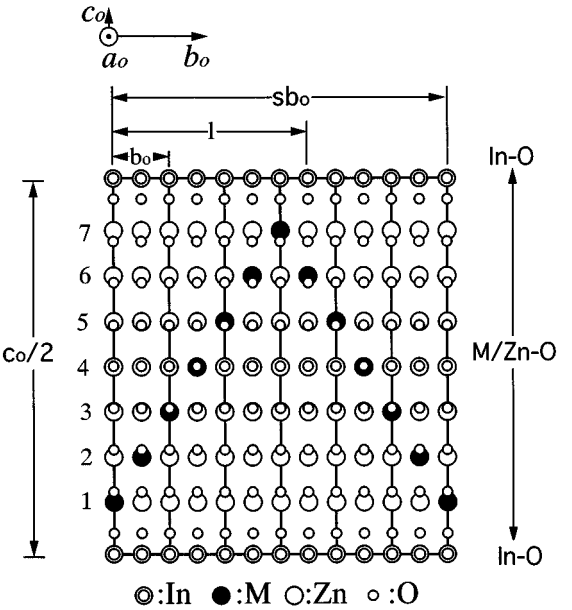

FIG. 10. Modulated structure model of $InMO_3(ZnO)_6$ (M = In). The trivalent In atoms are ordered to form a single In–O layer showing the zig-zag shape.

4. CONCLUSION

Modulated structures appearing in the homologous compounds $In_2O_3(ZnO)_m$ were observed by transmission electron microscopy and interpreted by a four-dimensional superspace groups. It is shown that the subcell structures for compounds of m = odd and even numbers can be described by monoclinic and orthorhombic cells, respectively. The extra spots are successfully analyzed by a one-dimensional modulation wave, where it can be represented by $ha^* + kb^* + lc^* + mq$. Based on the extinction rules and the lattice image observation, the possible superspace groups are assigned as P_s^{C2}, $P_{\bar{1}}^{Cm}$, and $P_{s\bar{1}}^{C2/m}$, for odd m numbers and $P_{1\bar{1}1}^{Cm2_1}$, and $P_{1\bar{1}s}^{Ccmm}$ for even m numbers, respectively.

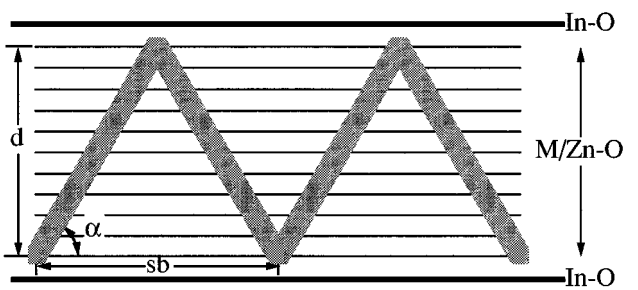

FIG. 11. Schematic model for the modulated structure showing the relation of the nonintegral periodicity of the modulated structure *sb*, the width of the M/Zn–O layer *d*, and the angle α of the zig-zag shape with the In–O layer.

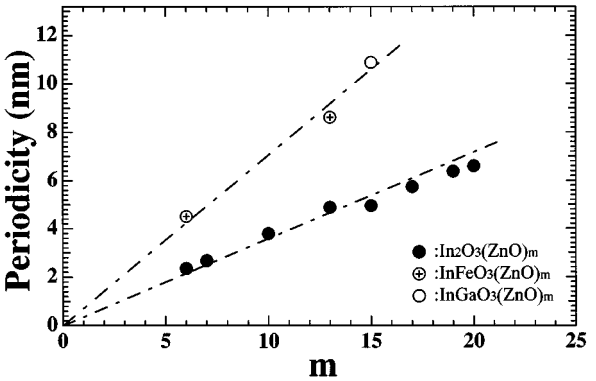

FIG. 12. Nonintegral periodicity of the modulated structure versus m values for various homologous compounds.

The dependence of the nonintegral periodicity of the modulation wave on the kind of M ion in M/Zn–O layers is also discussed.

REFERENCES

1. P. J. Cannard and R. J. D. Tilley, *J. Solid State Chem.* **73,** 418 (1998).
2. H. Kasper, *Z. Anorg. Allg. Chem.* **349,** 113 (1967).
3. N. Kimizuka, T. Mohri, and M. Nakamura, *J. Solid State Chem.* **81,** 70 (1989).
4. M. Nakamura, N. Kimizuka, and T. Mohri, *J. Solid State Chem.* **86,** 16 (1990).
5. M. Nakamura, N. Kimizuka, and T. Mohri, *J. Solid State Chem.* **93,** 298 (1991).
6. M. Nakamura, N. Kimizuka, T. Mohri, and M. Isobe, *J. Solid State Chem.* **105,** 535 (1993).
7. N. Kimizuka, M. Isobe, M. Nakamura, and T. Mohri, *J. Solid State Chem.* **103,** 394 (1993).
8. M. Nakamura, N. Kimizuka, T. Mohri, and M. Isobe, *J. Alloys Compds.* **192,** 105 (1993).
9. N. Kimizuka, M. Isobe, and M. Nakamura, *J. Solid State Chem.* **116,** 170 (1995).
10. M. Isobe, N. Kimizuka, M. Nakamura, and T. Mohri, *Acta Crystallogr. Sect. C* **50,** 332 (1994).
11. N. Uchida, Y. Bando, M. Nakamura, and N. Kimizuka, *J. Electron Microsc.* **43,** 146 (1994).
12. Y. Bando, Y. Kitami, K. Kurashima, T. Tomita, T. Honda, and Y. Ishida, *Microbeam Anal.* **3,** 279 (1994).
13. C. Li, Y. Bando, M. Nakamura, and N. Kimizuka, *J. Electron Microsc.* **46,** 119 (1997).
14. P. M. DE. Wolff, T. Janssen, and A. Janner, *Acta Crystallogr. Sect. A* **37,** 625 (1981).
15. P. M. DE. Wolff, *Acta Crystallogr. Sect. A* **33,** 493 (1977).
16. A. Janner, T. Janssen, and P. M. DE. Wolff, *Acta Crystallogr. Sect. A* **39,** 658 (1983).
17. A. Yamamoto, T. Janssen, A. Janner, and P. M. DE. Wolff, *Acta Crystallogr. Sect. A* **41,** 528 (1985).
18. A. Yamamoto, *Acta Crystallogr. Sect. A* **52,** 509 (1996).
19. R. D. Shannon RD, *Acta Crystallogr. Sect. A* **32,** 751 (1976).